Cancer vaccine strategies to improve immunotherapy: many roads lead to Rome

Tondini, E.

2

SELF-ADJUVANTING CANCER VACCINES FROM CONJUGATION-READY LIPID A ANALOGUES AND SYNTHETIC LONG PEPTIDES

Reintjens NRM*, Tondini E*, de Jong AR, Meeuwenoord NJ, Chiodo F, Peterse E, Overkleeft HS, Filippov DV, van der Marel GA, Ossendorp F, Codée JDC

J Med Chem. 2020; 63(20):11691-11706

*equal contribution

ABSTRACT

Self-adjuvanting vaccines, wherein an antigenic peptide is covalently bound to an immunostimulating agent, have been shown to be promising tools for immunotherapy. Synthetic Toll-like receptor (TLR) ligands are ideal adjuvants for covalent linking to peptides or proteins. We here introduce a conjugation-ready TLR4-ligand, CRX-527, a potent powerful lipid A analogue, in the generation of novel conjugate-vaccine modalities. Effective chemistry has been developed for the synthesis of the conjugation-ready ligand as well as the connection vaccine modality that proved to be potent in activation of dendritic cells, in facilitating antigen presentation and in initiating specific CD8+ T cell-mediated killing of antigen-loaded target cells in vivo. Synthetic TLR4-ligands thus show great promise in potentiating the conjugate vaccine platform for application in cancer vaccination.

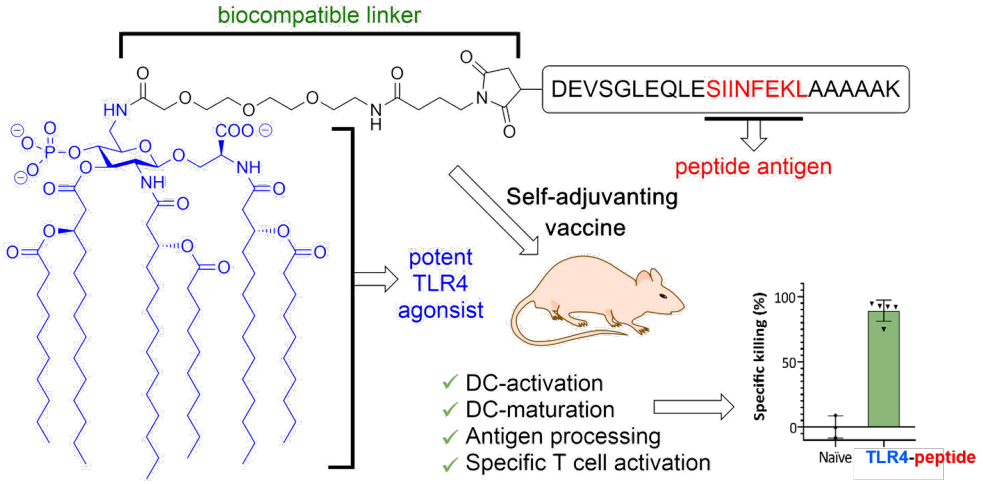

INTRODUCTION

Immunotherapy has become a powerful strategy to combat cancer. Significant advances have been made in the activa tion of anti-tumor T cell immunity, including the development of immune checkpoint blockade antibodies[1], chimeric antigen receptor T cells (CAR T cells)[2] and vaccination strategies, in which the immune system is trained to recognize cancer neoantigens.[3,4] To optimally direct an immune reaction against cancer via vaccination, adjuvants are used to activate antigen-presenting cells, such as dendritic cells (DCs) and macrophages. DCs express pathogen recognition receptors (PRRs)[5], through which they recognize invading pathogens and initiate an immune response, which eventually leads to the priming of T cells.[6]

Pathogen associated molecular patterns (PAMPs) are ligands for these PRRs and can be used as molecular-adjuvants. Molecular-adjuvants are well-defined single molecule immunostimulants that act directly on the innate immune system to enhance the adaptive immune response against antigens. Many well-defined PAMPs have been explored over the years, and the most extensively targeted PRR-families are the Toll-like receptors (TLRs)[7], C-type lectins[8], and Nucleotide-binding Oligomerization Domain (NOD)-like receptors[9,10]. To further improve vaccine activity, the antigen and adjuvants have been combined in covalent constructs, delivering "self-adjuvanting" vaccine candidates.[11,12] In the immune system, the stimulation of different TLRs can activate distinct signaling cascades and thereby support the generation of polarized types of immune reactions. Hence, targeting of distinct TLRs in vaccination influences the nature of the adaptive immune response induced.[13,14].

Several TLR agonists[11,15,16] have been conjugated to antigenic peptides (often synthetic long peptides, SLPs), including ligands for TLR2,[17–22] TLR7,[23,24] and TLR9,[20,2 5,26] yielding vaccine modalities with improved activity with respect to their non-conjugated counterparts. Lipid A (**Figure 1A**), a conserved component of the bacterial cell wall, is one of the most potent immune-stimulating agents known to date and it activates the innate immune system through binding with TLR4. The high toxicity of lipid A makes it unsuitable for safe use in humans, but monophosphoryl lipid A (MPLA, **Figure 1A**), a lipid A derivative in which the anomeric phosphate has been removed, has proven its effectiveness as an adjuvant in various approved vaccines.[27–29] It has also been used recently in conjugates in which it was covalently attached to a tumor-associated carbohydrate antigen (TACA) or a synthetic bacterial glycan.[30–34] The latter conjugate was able to elicit

a robust IgG antibody response in mice, critical for effective anti-bacterial vaccination.[34] MPLA thus represents a very attractive PAMP to be explored in SLP conjugates, targeting cancer epitopes. The physical properties and challenging synthesis of lipid A derivatives, however, limit its accessibility.[35–37] Because of its potent immunostimulating activity, many mimics of MPLA have been developed and the class of aminoalkyl glucosamine 4-phosphates (AGPs) has been especially promising.[38–41] AGPs have been shown to be efficacious adjuvants and to be clinically safe, resulting in their use in a Hepatitis B vaccine.[42] CRX-527 (**Figure 1A**) has been established as one of the most potent AGPs.[38]

We here introduce conjugation-ready derivatives of CRX-527 for application in the development of adjuvant-SLP vaccines conjugates. We have established a robust synthetic route to generate linker-equipped CRX-527 analogues and used these in the assembly of SLP conjugates. The self-adjuvanting SLPs carrying this TLR4-ligand are capable of mobilizing a strong T cell immune response against the incorporated antigen and are capable of promoting effective and specific killing of target cells expressing the antigen *in vivo*.

RESULTS AND DISCUSSION

Synthesis of the ligands and conjugates.

In the development of the conjugation-ready CRX-527-derivates we set out to probe both the influence of the nature of the linker and the mode of connectivity of the linker to the TLR4-ligand, CRX-527 (See **Figure 1B**). In lipopolysaccharides bacterial *O*-antigens are connected to a lipid A anchor through the C6-position of the glucosamine-C4-phosphate residue and from the crystal structure of lipid A in complex to the TLR4-MD2 complex, it is apparent that this position is exposed from the complex.[43] The C6-position of the glucosamine-C4-phosphate can thus be used for conjugation purposes. Indeed, previous work on anti-bacterial MPLA conjugate vaccines has shown that the adjuvant can be modified at this position without compromising adjuvant activity.[34] We explored two types of linkers at the C6-position of CRX-527: a hydrophobic alkyl linker (**A**) and a hydrophilic triethylene glycol (TEG) linker (**B**). These linkers were connected to CRX-527 through an ester bond,[34] or *via* a more stable amide bond. To connect the ligands to the SLPs, the linkers were equipped with a maleimide, to allow for a thiol-ene conjugation to the sulfhydryl functionalized SLP. We used the ovalbumin derived SLP, DEVSGLEQLESIINFEKLAAAAAK ($DEVA_5K$) as a model antigen.[20] Herein, the MHC-I epitope SIINFEKL is embedded in a longer peptide motif to

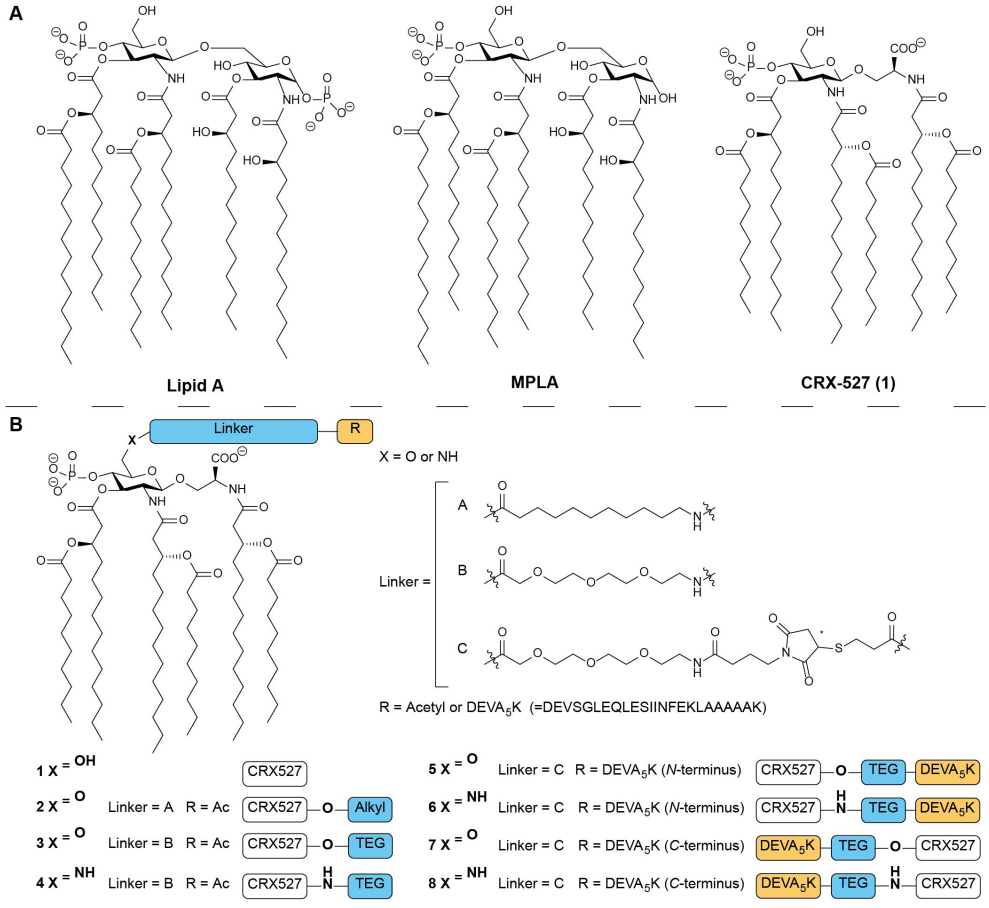

Figure 1. (A) Representative structures of lipid A of *E. coli* and MPLA of *Salmonella enterica* serotype minnesota Re 595; Structure of CRX-527 (1). (B) Structures of CRX-527 derivatives 2-4 and CRX-527 conjugates 5-8. The $DEVA_5K$ peptide in the conjugates carries the SIINFEKL epitope in its sequence.

ensure that the peptide will have to undergo proteasomal processing to produce the minimal epitope. The target compounds generated for thy are depicted in **Figure 1** and include CRX-527 (**1**), ester-linker CRX-527 **2** and **3**, amide-linker CRX-527 **4** as well as the conjugates **5** and **6** having the CRX-527 ligand at the *N*-terminus of the peptide and conjugates **7** and **8**, with the ligand at the *C*-terminus of the SLP. To obtain CRX-527 derivatives **1**-**4**, building blocks **16a/b** were required and the assembly of these key intermediates was accomplished as depicted in **Figure 2A**. Based on the synthesis route to CRX-527 developed by Johnson and co-workers[41], we assembled glucosaminyl serine building block **11** from glucosamine donor **9** and serine **10**. Condensation of **9** and **10** under the

influence of boron trifluoride etherate proceeded in a completely β-selective manner to give a mixture of the desired product and unreacted donor **9**. The mixture could be separated after hydrogenolysis of the benzyl ester giving acid **11** in 63% yield on 170 mmol scale. Next, all acetyls were removed, before the benzyl ester was re-installed using phase transfer conditions to deliver triol **12**. To enable the introduction of the chiral lipid tail we masked the C4- and C6-hydroxyl groups in **12** with a silylidene ketal. This protecting group strategy proved to be crucial as the use of a C6-O-*tert*-butyldimethylsilyl (TBDMS) group as previously reported,[41] led to an intractable mixture when the lipid tails were attached. As lipid A analogues bearing fewer lipid tails may have a different immunological response[44], the purity of the ligand is of utmost importance. Next, the Troc-protecting groups were removed from both amine groups, after which an *N*,*N*,*O*-triacetylation event using fatty acid **14** (Supporting information Scheme 1) and EDC·MeI and catalytic DMAP (0.03 eq.) delivered compound **15**. On a 9.5 mmol scale this intermediate was obtained in 57% over two steps. The silylidene ketal was removed, and then the primary alcohol was selectively protected with a TBDMS group, and the phosphate triester was installed at the C4-OH. Desilylation provided key building block **16a** on a multi-gram scale. The alcohol in **16a** was transformed into the corresponding primary azide using Mitsunobu conditions delivering **16b**.

With building blocks **16a/b** available in sufficient amounts, attention was directed to the assembly of ligands **1**-**4,** having either an alkyl or triethylene glycol (TEG) linker (**Figure 2B**). Debenzylation of **16a** using Pd/C gave the original CRX-527 (**1**). Elongation of **16a** with the *N*-acetylated linkers **17** or **18**, under the influence of EDC·MeI and DMAP, furnished the fully protected linker-CRX-527 compounds that were subjected to a hydrogenation reaction to obtain ligands **2** and **3**. In contrast to the findings of Guo and coworkers, in their synthesis of linker functionalized MPLA derivatives, where the C6-ester bond was found unstable,[34] no hydrolysis of esters **2** and **3** was observed. Ligand **4** was obtained from azide **16b** by zinc mediated reduction, condensation with linker **18** and subsequent hydrogenation.

Next, the synthesis of the CRX-527-peptide conjugates **5**-**8** was undertaken (**Figure 2C**). Based on the immunological evaluation of the ligands **1**-**4** (*vide infra*, **Figure 3**) the TEG linker was used for the assembly of the peptide antigen conjugates. First, **16a** and azido linker **19** were conjugated under the agency of EDC.

Reduction of the azide and benzyl esters was then followed by the introduction

of the maleimide functionality using sulfo-*N*-succinimidyl 4-maleimidobutyrate to give conjugation-ready CRX-527 **20a**. The amide congener of this compound was assembled from **16b** in an analogous manner. The $DEVA_5K$-peptides with a thiol function at the *N*-terminus (**21**) or the *C*-terminus (**22**) were assembled using a semi-automated solid phase peptide synthesis protocol and purified to homogeneity by RP-HPLC (See Supporting information for full synthetic details). The conjugation of the ligand and the peptide-antigen required significant optimization because of the physical properties of the ligand and the peptides. We found that the thiol-maleimide coupling could be achieved by dissolving **21** or **22** in DMF/H_2O (4/1 v/v) followed by the addition of a solution of maleimide **20a** or **20b** in $CHCl_3$. After shaking for two days, LC-MS analysis confirmed the full conversion of the maleimide and the conjugates were purified by C18 column chromatography (See Supporting information for details). **Figure 2D** shows the analysis of the conjugation of maleimide **20a** with an excess of thiol **22**, providing conjugate **7** (**Figure 2D**, left panel), which was purified by HPLC to provide the pure conjugate (**Figure 2D**, middle panel). The integrity and purity of the synthesized *N*-terminus conjugates **5** and **6**, and *C*-terminus conjugates **7** and **8** were ascertained by LC-MS analysis and MALDI-TOF MS (See **Figure 2D**, right panel for the MALDI-TOF MS spectrum of **7**).

In vitro activity.

Immunological evaluation of TLR4-ligands **1**-**4** and conjugates **5**-**8** was performed by first assessing their ability to induce maturation of dendritic cells and to present antigen to T cells *in vitro*. Binding of the lipid A to the TLR4/MD-2 complex triggers the production of inflammatory cytokines and maturation of the DCs. Production of the subunit IL-12p40 of the pro-inflammatory cytokine IL-12 is a marker of this activation. We first analyzed if the addition of the peptide would affect the interaction with TLR4 and impede the activity of the ligand. To probe activation of the DCs by the CRX-527-ligands and conjugates, murine DCs were stimulated for 24h with the different compounds and the amount of IL-12p40 in the supernatant was measured. First, the effect of the different linkers (compounds **2**-**4**) on the activity of the CRX-527 ligand was evaluated. As can be seen in **Figure 3A**, stimulation of the DCs with the CRX-527 ligand **1** induces strong IL-12p40 secretion and its activity is higher than the commercially available TLR4-ligand MPLA. The addition of an ester-alkyl linker (**2**) significantly decreased the ability of the ligand to induce DC-activation.

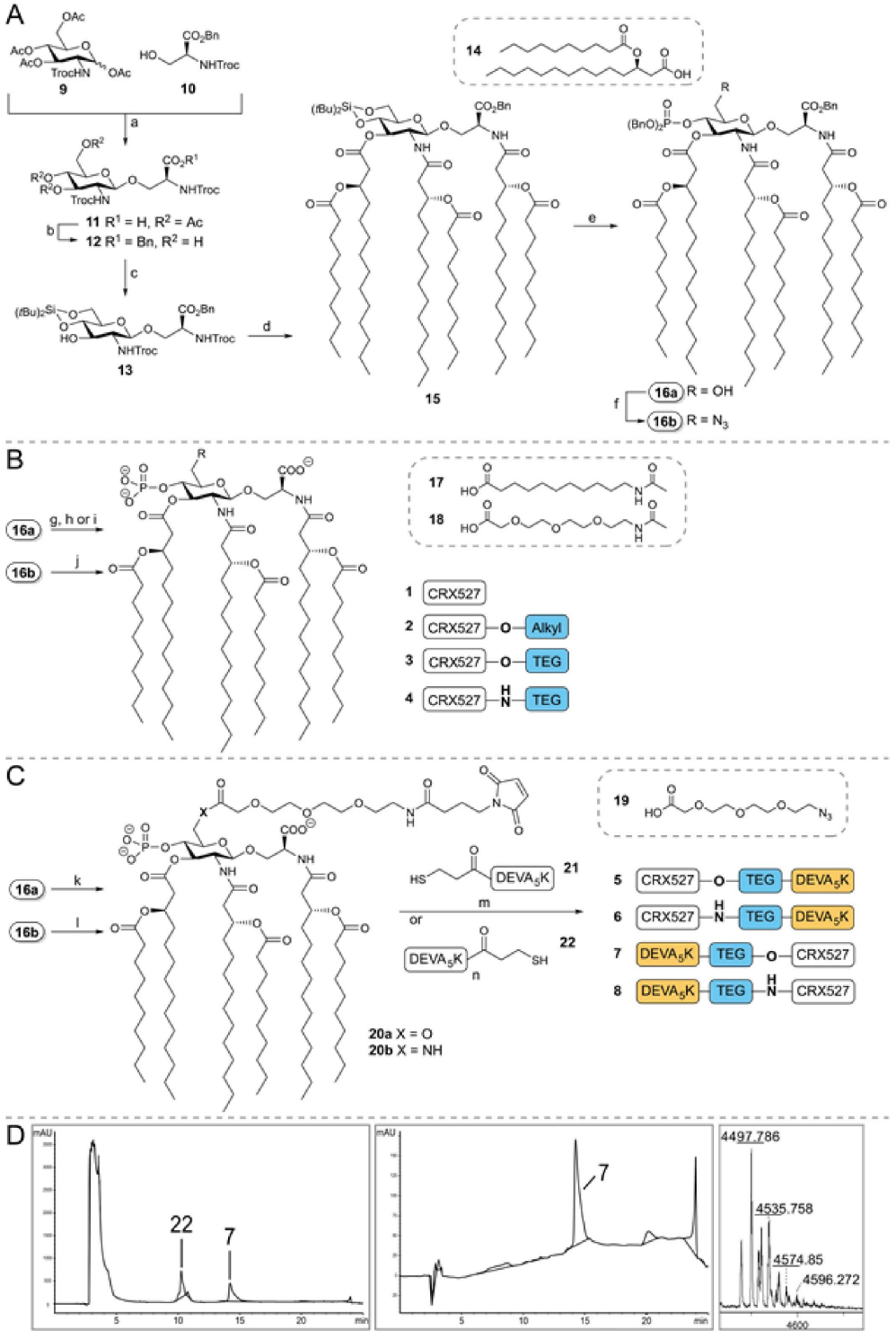
A
9
10
14
11 R1 = H, R2 = Ac
12 R1 = Bn, R2 = H
13
15
16a R = OH
16b R = N3
B
16a
16b
17
18
1 CRX527
2 CRX527 O Alkyl
3 CRX527 O TEG
4 CRX527 H N TEG
C
16a
16b
19
21
22
or
20a X = O
20b X = NH
5 CRX527 O TEG DEVA5K
6 CRX527 H N TEG DEVA5K
7 DEVA5K TEG O CRX527
8 DEVA5K TEG H N CRX527
D
mAU
22
7
min
4497.786
4535.758
4574.85
4596.272
4600

Figure 2. (A) Synthesis of building blocks **16a/b**. *Reagents and conditions*: a) *i.* $BF_3{\cdot}OEt_2$, DCM, 0°C to rt; *ii.* H_2, Pd/C, THF, 63% over two steps; b) *i.* NH_4OH, MeOH; *ii.* BnBr, TBAB, DCM/$NaHCO_3$ (aq. sat.), 79% over two steps; c) $(t\text{Bu})_2Si(OTf)_2$, DMF, -40°C, 94%; d) *i.* Zn dust, AcOH; *ii.*) **14**, EDC·MeI, DMAP, DCM, 57% over two steps. e) *i.* $HF{\cdot}Et_3N$. THF, 0°C, 92%; *ii.* TBDMSCl, pyridine, 88%; *iii.* dibenzyl *N*,*N*-diisopropylphosphoramidite, tetrazole, DCM, 0°, 1h; *iv.* 3-chloroperbenzoic acid, quant. over two steps; *v.* TFA, DCM, 84%. f) PPh_3, DEAD, DPPA, THF, 67%; (B) Synthesis of TLR4-ligands **1**-**4**. *Reagents and conditions*: g) H_2, Pd/C, THF, **1**: 89%; h) *i.* **17**, EDC·MeI, DMAP, DCE, 88%; *ii.* H_2, Pd/C, THF, **2**: 56%; i) *i.* **18**, EDC·MeI, DMAP, DCE, 74%; *ii.* H_2, Pd/C, THF, **3**: 66%; j) *i.* Zn, NH_4Cl, DCM/MeOH/H_2O; *ii.* **18**, EDC·MeI, DMAP, DCE, 40% over two steps; *iii.* H_2, Pd/C, THF, **4**: 61%; (C) Assembly of conjugates **5**-**8**. *Reagents and conditions*: k) *i.* **19**, EDC·MeI, DMAP, DCE, 80%; *ii.* H_2, Pd/C, THF, 77%; *iii.* sulfo-*N*-succinimidyl 4-maleimidobutyrate sodium salt, Et_3N, DCM, **20a**: 84%. l) *i.* Zn, NH_4Cl, DCM/MeOH/H_2O; *ii.* **19**, EDC·MeI, DMAP, DCE, 56% over two steps; *iii.* sulfo-*N*-succinimidyl 4-maleimidobutyrate sodium salt, Et_3N, DCE, **20b**: 81%; m) **21**, DMF/$CHCl_3$/H_2O, 48h, **5**: 52%, **6**: 54%; n) **22**, DMF/$CHCl_3$/H_2O, 48h, **7**: 57%, **8**: 42%. (D) LC-MS trace of crude and purified *C*-terminus conjugate **7**, and MALDI analysis of **7**.

However, the ester- or amide-TEG linker functionalized ligands mostly preserve the induction of IL-12p40, as shown for compounds **3** and **4**. For these two ligands, the activity was comparable to the unmodified ligand **1** up to 1.56 nM, and slightly reduced at the lowest concentrations. However, substantial levels of IL-12p40 could still be detected at these concentrations. Possibly, the hydrophobic nature of the alkyl linker of compound **2** induces a different configuration of the ligand that affects binding to the MD-2/TLR4 pocket, preventing activation of the signaling cascade[43]. The DC-activating capacity of compounds **1**, **3** and **4** indicates that functionalization at the C6-position with a hydrophilic linker does not inhibit binding of the ligand to the receptor.

Next, the $DEVA_5K$ peptide conjugates **5**-**8** were evaluated for their ability to induce IL-12p40 in DCs (**Figure 3B**). We analyzed whether conjugation of the peptide via the ester- (compounds **5** and **7**) or the amide-TEG linker (compounds **6** and **8**) could differently modulate the activity of the conjugates. Moreover, we investigated whether conjugation of the ligand to the *N*- or *C*-terminus of the peptide could also influence activity. Interestingly, we found that even if ligands **3** and **4** do not display any differences in activity (**Figures 3A** and **3B**), their respective peptide conjugates show differential potencies (**Figure 3B**). Specifically, the ester conjugates **5** and **7** induce high levels of IL-12p40, similarly to the ligands **3** and **4**, while the amide conjugates **6** and **8**, display overall lower levels of IL-12p40 production. No difference in activity was observed between the *N*- or *C*-terminal $DEVA_5K$ conjugates. The activity of the ester conjugates **5** and**7** titrates faster than the free ligands, **3** and **4**, as can be observed at the lowest concentrations.

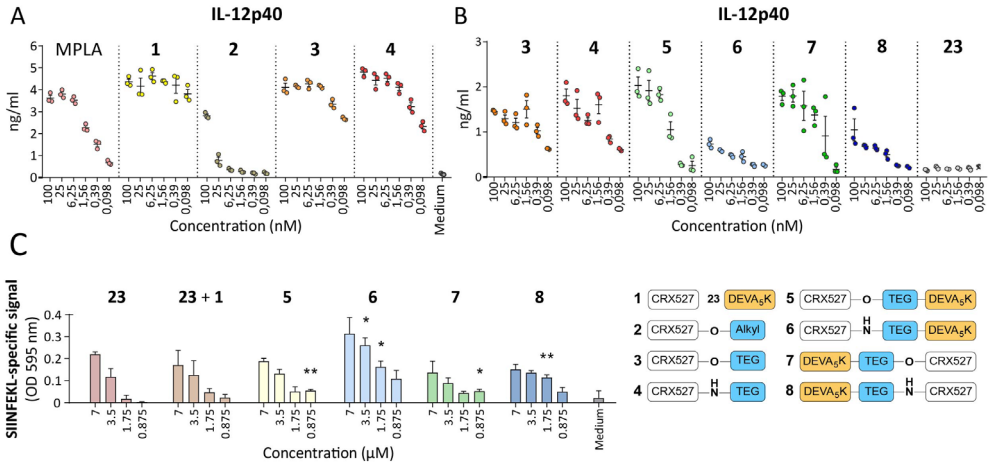

Figure 3. The TLR4-ligands and the cognate conjugates induce IL-12 production and T cell activation in vitro. (A) The D1 dendritic cell line was stimulated for 24 hours with the synthetic compounds 1-4 and the induction of DC maturation was analyzed by measuring IL-12p40 production. MPLA was included as a control for TLR4 stimulation (B) The activity of the conjugates 5-8 together with their reference ligands 3 and 4 was analyzed by measuring IL-12p40 production. Unconjugated peptide was included as negative control. (C) Antigen uptake and presentation was measured by incubation of compound-pulsed D1 with the SIINFEKL-specific hybridoma T cell line B3Z. B3Z activation was determined by colorimetric reaction of the CPRG reporter enzyme and measurement of absorbance.

These data show that conjugation of CRX-527 to a long peptide via different linkers results in immunologically active compounds and has therefore potential for vaccination. Importantly, the efficacy of peptide vaccines relies on the ability of DCs to take up the peptide and process it to enable surface presentation of the epitope on MHC molecules. Recognition of the antigen-MHC complex by the T cell receptor and simultaneous co-stimulation by mature DCs then results in the initiation of a T cell response.[45] The uptake and processing of the conjugates **5**-**8** was evaluated in an antigen presentation assay using the T cell hybridoma reporter line B3Z, which is specific for the SIINFEKL epitope contained in the $DEVA_5K$ peptide. The B3Z cell line possesses a T cell receptor, specific for the SIINFEKL epitope, which controls the expression of the beta-galactosidase reporter gene. Recognition of the SIINFEKL epitope induces the expression of the enzyme, which can subsequently be detected through a colorimetric reaction caused by the conversion of a substrate. The efficiency in antigen presentation of the conjugates was compared to free peptide **23** and to a mixture of peptide **23** and CRX-527 ligand **1**. **Figure 3C** shows that incubation of DCs with the

ester conjugates **5** and **7**, leads to similar levels of T cell activation as the free peptide and the mixture of the peptide and CRX-527 **1**. Therefore, conjugation of the peptide to the CRX-527 ligand does not affect its uptake and processing, both after *N*-terminus and *C*-terminus conjugation. Notably, incubation with the amide conjugates **6** and **8** resulted in slightly enhanced antigen presentation. In this case, the *N*-terminus conjugate **6** displayed higher antigen presentation and consequent T cell activation than its *C*-terminal counterpart. It is possible that hydrolysis takes place for the ester conjugates **5** and **7** prior to uptake in the DCs, leading to diminished uptake of the peptide moiety (as compared to their amide counterparts) and resulting in lower antigen presentation. Importantly, this read-out system is not influenced by the co-stimulatory signals provided by mature DCs, and only reports whether uptake and processing occur in DCs.

To summarize, in vitro evaluation of the conjugates revealed that the ester conjugates display higher potency in inducing DC maturation, while the amide conjugates are presented more efficiently. Therefore, the combined action of co-stimulation, induced by the triggering of the TLR4 and antigen presentation to CD8+ T cells was evaluated in an *in vivo* immunization study.

In vivo activity.

Having established that the conjugates maintained the capacity to activate DCs and to induce antigen presentation, the conjugated vaccines were compared for their ability to induce *de novo* T cell responses *in vivo*. Mice were injected intradermally with 5 nmol each of conjugates **5**-**8**, or a mixture of peptide **23** and TLR4-ligand **1**, and the presence of SIINFEKL-specific T cell responses was monitored in blood via SIINFEKL-Kb tetramer staining. Analysis of blood after the first vaccine injection demonstrated the successful induction of SIINFEKL-specific T cell responses in all groups vaccinated with the CRX-527 conjugates. No significant differences could be distinguished between the groups (Supporting information Figure 1A). Two weeks after the first injection, mice were boosted with the same formulations and the SIINFEKL-specific responses were measured in blood 7 days later. As shown in **Figure 4A** and **B**, the strongest induction of SIINFEKL-specific $CD8^+$ T cells was detected in the group that received the *N*-terminal ester conjugate **5**. Overall, the two *N*-terminal conjugates **5** and **6** displayed higher T cell induction than their *C*-terminal counterpart conjugates **7** and **8**. T cell responses were detectable also in mice vaccinated with a mixture of CRX-527 and peptide, however, these responses displayed a higher spread than all conjugate groups. One day later, the spleens and lymph nodes draining

the vaccination site were harvested to analyze the presence and the phenotype of the SIINFEKL-specific responses in these organs. Analysis of T cell responses in the spleen displayed a similar trend to that observed in blood (Supporting information Figure 1B). However, in the inguinal lymph nodes (**Figure 4C**) a higher percentage of SIINFEKL-specific T cell responses was detected for the *N*-terminal conjugates **5** and **6**. In this organ, mice vaccinated with the *C*-terminus conjugates **7** and **8** or the mixture display low T cell responses. Next, we investigated whether the phenotype of the SIINFEKL-specific T cells induced by the *N*-terminal conjugates **5** and **6** was different compared to the group that was vaccinated with the mixture of TLR4-ligand **1** and peptide **23**. The induction of differentiation into memory $CD127^{+}/KLRG1^{low}$ responses is a marker for T cell quality, which is associated with improved functions and tumor clearance.[46] This phenotype was pronounced in the groups vaccinated with the conjugates **5** and **6** and was clearly less present in the group that was vaccinated with the mixture (**Figure 4D**). Within the T cell memory population, two further subsets can be distinguished based on the expression of CD62L, a surface protein that, when present, determines homing at lymphoid tissues, rather than circulation in the blood vessels and tissues. High expression of CD62L defines central memory T cells, while lower expression of this surface protein determines effector memory T cells. This last subset recirculates in tissues and can exert immediate effector functions upon antigen reencounter. We observed significantly higher differentiation into effector memory T cells when mice were immunized with the conjugated vaccines **5** and **6** rather than the mixture (**Figure 4E**). It has been shown that the promotion of differentiation into effector memory T cells rather than short-lived effector cells is dependent on optimal priming conditions, such as the presence of helper T cells[46–48] and proper co-stimulatory signals[49,50]. These data indicate that conjugation of the TLR4-adjuvant and peptide represents an effective strategy to achieve an increased effector memory T cell phenotype, which is an important hallmark for effective vaccination.[51–53]

Finally, we investigated the functionality of the induced T cell responses upon vaccination with conjugate **6** in an *in vivo* cytotoxicity assay. Mice were immunized with the *N*-terminus conjugate **6**, and the kinetics of the T cell response was followed in blood by SIINFEKL-Kb tetramer staining (**Figure 5A**). After 14 days a boost was administered, and one week later animals were intravenously injected with cells loaded with either SIINFEKL peptide or an irrelevant peptide, to measure the ability of the induced T cells to specifically kill SIINFEKL-loaded

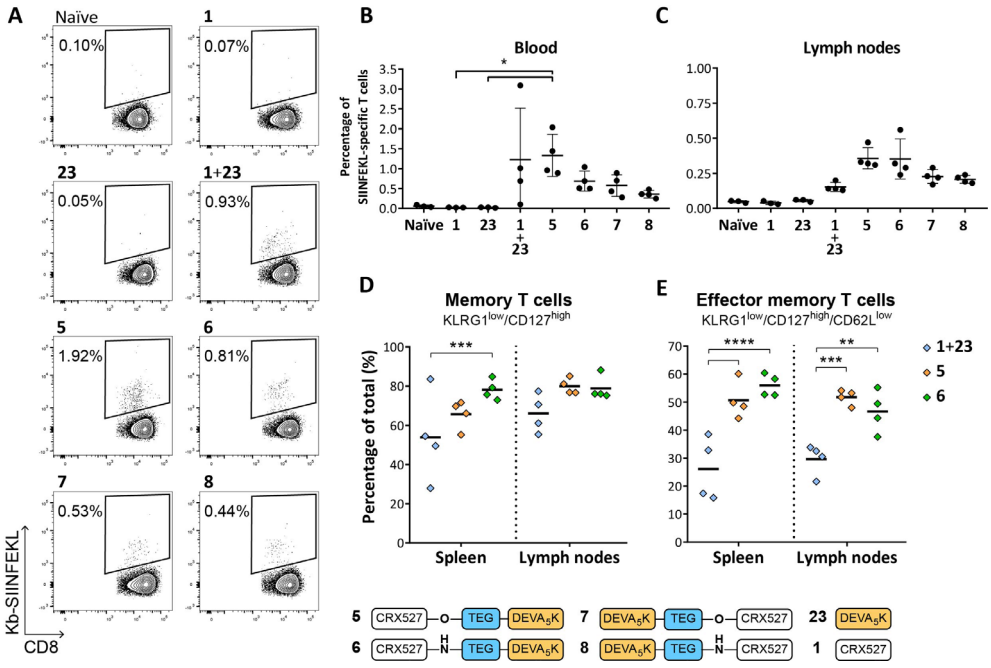

Figure 4. The conjugates induce SIINFEKL-specific T cell responses with an effector memory phenotype *in vivo*. (A) Representative plots of SIINFEKL-Kb tetramer positive T cells in blood of vaccinated mice. (B) Percentage of SIINFEKL-specific T cell responses measured by tetramer staining in blood at day 21 after booster vaccination. Every dot represents a single animal. (C) At day 22, inguinal lymph nodes were harvested and the presence of SIINFEKL-specific T cells was measured by tetramer staining in all groups. Statistical significance was determined by Kruskal-Wallis test followed by multiple comparison rank test and Dunn's correction, * $p < 0.05$. (D and E) The phenotype of SIINFEKL-specific T cells was characterized in the higher-responding groups in spleen and lymph nodes by analyzing the expression of the surface markers KLRG1, CD127 (D) and CD62L (E) by flow cytometry. Statistical significance was determined by two-way ANOVA followed by multiple comparison and Tukey correction, ** $p < 0.01$ *** $p < 0.001$, **** $p < 0.0001$.

cells. Prior to injection, the two groups of target cells were differentially labelled with the fluorescent dye CFSE, to be able to distinguish the two populations during later analysis by flow cytometry. After 18 hours, the spleens were harvested and the killing of the two peptide-loaded populations was determined in naïve and vaccinated mice via flow cytometric analysis. (**Figure 5A** and **B**). As expected, naïve mice displayed similar relative frequencies of the two CFSE-labelled populations. On the contrary, specific killing of the SIINFEKL-loaded target cells was observed in the vaccinated mice. Notably, four out of five mice that were vaccinated with conjugate **6** displayed > 90% killing. The killing degree

reflected the levels of specific $CD8^+$ T cells present, as detected in the inguinal lymph nodes by tetramer staining (**Figure 5C**).

To conclude, *in vivo* evaluation of the CRX-527-peptide conjugates shows that conjugates **5**-**8** are effective in initiating antigen-specific T cell responses. In particular, the *N*-terminus conjugates could raise higher responses than their C-terminal counterparts. Phenotypic and functional analysis of these responses revealed that CRX-527 conjugate **6** was capable of raising an adequate protective immune response, effectively killing cells presenting the antigen against which the vaccination was directed and underscoring the potential of these new conjugates for anti-cancer immunotherapy.

CONCLUSIONS

Adjuvant-antigen conjugates are promising agents for cancer immunotherapy. Well-defined molecular adjuvants are essential to stimulate relevant immune subsets and generate the most appropriate type of immunity against distinct tumor types. MPLA is one of the most potent innate immune-stimulating agents, which is currently used as an adjuvant in vaccines, but the application of this TLR4-ligand in adjuvant-antigen constructs is hampered by its challenging synthesis. CRX-527 is a potent MPLA analogue and we have here disclosed an expeditious synthesis of conjugation ready derivatives of this immune-stimulating agent and demonstrated the preparation of TLR4-ligand-peptide antigen conjugates for the first time. The assembly of the conjugation-ready ligand critically depended on the protecting group strategy and the use of a silylidene ketal in the glucosaminyl serine proved crucial for the efficient introduction of the lipid tails. The developed route of synthesis is high-yielding and could be executed on a multigram scale to allow the generation of several peptide conjugates. Different linker systems and connection modes were probed to conjugate the TLR4-ligand to a synthetic long peptide antigen. *In vitro* evaluation of the conjugates showed that the attachment of a lipophilic linker at the C6 of CRX-527 abrogates the activity of the ligand. The use of a hydrophilic glycol-based linker provided conjugates which could induce strong DC maturation, and allowed effective antigen processing and presentation. *In vivo* evaluation of the conjugates demonstrated the efficacy of the vaccine modalities in priming *de novo* $CD8^+$ T cell responses. Conjugation of the TLR4-ligand at the *N*-terminus of the peptide stimulated the best induction of T cell responses, promoting differentiation into effector memory T cell responses. Finally, it was shown that the CRX-527-pep

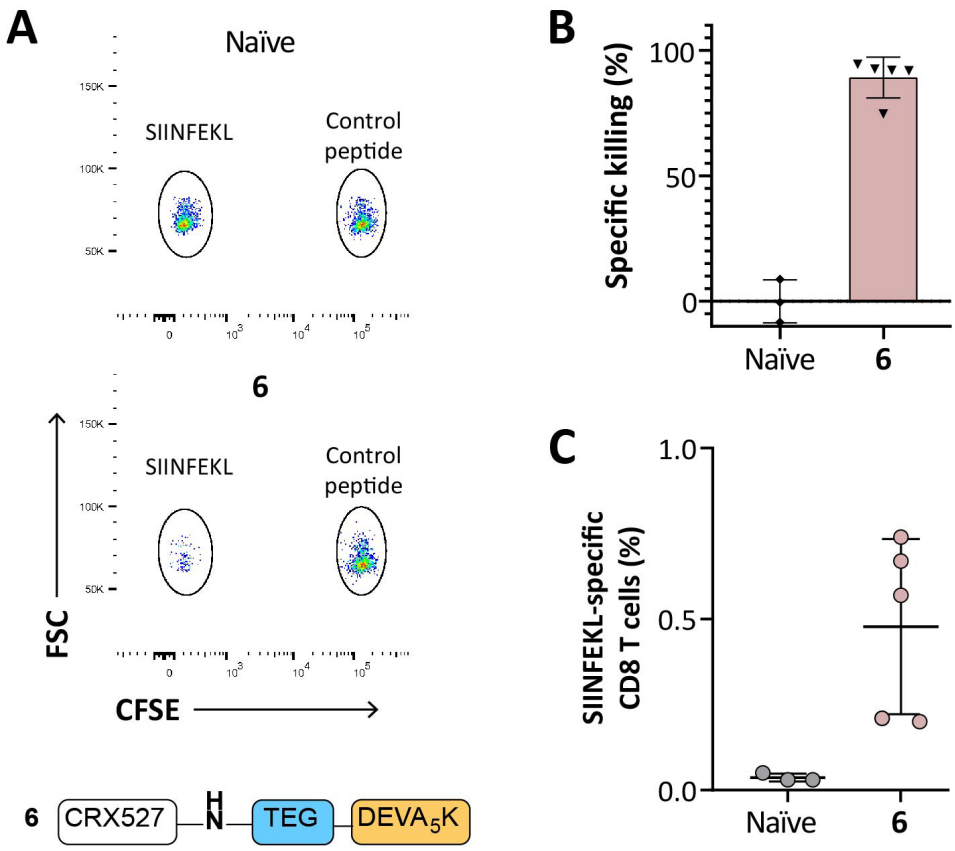

Figure 5. Immunization with CRX-527 conjugate **6** results in efficient specific killing of peptide-loaded target cells. Naïve C57BL/6 mice (n=5) were injected intradermally with 5 nmol of CRX-527 conjugate. (A**)** After booster vaccination, mice were injected with differentially CFSE-labelled target cells. 18 hours after injection, spleens were analyzed for the presence of the two CFSE-labelled target populations. (B**)** Calculated specific-killing of SIINFEKL-loaded cells. (C**)** The amount of SIINFEKL-specific T cells was determined in the lymph nodes by tetramer staining.

tide, in which the TLR4-ligand was conjugated to the *N*-terminus of the SLP through an amide linked spacer, was a potent inducer of antigen-specific effector $CD8^+$ T cell responses *in vivo*. Overall, we have developed a platform to potentiate synthetic peptide vaccines with a potent and well-defined TLR4-ligand, a powerful addition to the toolbox available to generate self-adjuvanting vaccines. CRX-527 conjugates hold great promise for the development of anti-cancer SLP-vaccines and the availability of the conjugation-ready ligand and chemistry to fuse the ligand to peptide antigens will enable the generation of conjugates bearing other peptide epitopes, such as defined oncoviral antigens or cancer

neoantigens. The generated conjugation-ready CRX-527 may also find application in the generation of well-defined anti-bacterial, viral or fungal vaccines.

EXPERIMENTAL SECTION

Materials and Methods. All reagents were of commercial grade and used as received unless stated otherwise. Reaction solvents were of analytical grade and when used under anhydrous conditions stored over flame-dried 3Å molecular sieves. All moisture and oxygen sensitive reactions were performed under an argon atmosphere. Column chromatography was performed on silica gel (Screening Devices BV, 40-63 µm, 60 Å). For TLC analysis, pre-coated silica gel aluminum sheets (Merck, silica gel 60, F254) were used with detection by UV-absorption (254/366 nm) where applicable. Compounds were visualized on TLC by UV absorption (245 nm), or by staining with one of the following TLC stain solutions: $(NH_4)_6Mo_7O_{24}{\cdot}H_2O$ (25 g/L), $(NH_4)_4Ce(SO_4)_4{\cdot}2H_2O$ (10 g/L) and 10% H_2SO_4 in H_2O; bromocresol (0.4 g/L) in EtOH; $KMnO_4$ (7.5 g/L), K_2CO_3 (50 g/L) in H_2O. Staining was followed by charring at ~150°C. ^{1}H, ^{13}C and ^{31}P NMR spectra were recorded on a Bruker AV-300 (300/75 MHz), AV-400 (400/100 MHz) spectrometer, a Bruker AV-500 Ultrashield (500/126 MHz) spectrometer, a Bruker AV-600 (600/151 MHz) or a Bruker AV-850 (850/214 MHz) and all individual signals were assigned using 2D-NMR spectroscopy. Chemical shifts are given in ppm (δ) relative to TMS (0 ppm) in $CDCl_3$ or via the solvent residual peak. Coupling constants (*J*) are given in Hz. LC-MS analysis were done on an Agilent Technologies 1260 Infinity system with a C18 Gemini 3 µm, C18, 110 Å, 50 x 4.6 mm column or a Vydac 219TP 5 µm Diphenyl, 150 x 4.6 mm column with a flow of 1, 0.8 or 0.7 ml/min. Absorbance was measured at 214 nm and 256 nm and an Agilent Technologies 6120 Quadrupole mass spectrometer was used as detector. Peptides, TLR2-ligand and conjugate were purified with a Gilson GX-281 preparative HPLC with a Gemini-NX 5u, C18, 110 Å, 250 x 10.0 mm column or a Vydac 219TP 5 µm Diphenyl, 250 x 10 mm column. Peptide fragments were synthesized with automated solid phase peptide synthesis on an Applied Biosystems 433A Peptide Synthesizer. Optical rotations were measured on an Anton Paar Modular Circular Polarimeter MCP 100/150. High resolution mass spectra were recorded on a Synapt G2-Si or a Q Exactive HF Orbitrap equipped with an electron spray ion source positive mode. Mass analysis of the TLR4-ligands and TLR4-ligand conjugates was performed on an Ultraflextreme MALDI-TOF or a 15T MALDI-FT-ICR MS system. Infrared spectra were recorded on a Perkin Elmer Spectrum 2 FT-IR. Unprotected lipid A derivatives were dissolved in a mixture of $CDCl_3$/MeOD 5/1 v/v for NMR analysis. DC activation and B3Z assay results were analysed with GraphPad Prism version

7.00 for Windows, GraphPad Software. Purity of all compounds is > 95% as determined by NMR or LC-MS analysis. FA = fatty acid.

Automated solid phase synthesis general experimental information. The automated solid-phase peptide synthesis was performed on a 250 µmol scale on a Protein Technologies Tribute-UV IR Peptide Synthesizer applying Fmoc based protocol starting from Tentagel S RAM resin (loading 0.22 mmol/g). The synthesis was continued with Fmoc-amino acids specific for each peptide. The consecutive steps performed in each cycle for HCTU chemistry on 250 µmol scale: 1) Deprotection of the Fmoc-group with 20% piperidine in DMF for 10 min; 2) DMF wash; 3) Coupling of the appropriate amino acid using a four-fold excess. Generally, the Fmoc amino acid (1.0 mmol) was dissolved in 0.2 M HCTU in DMF (5 mL), the resulting solution was transferred to the reaction vessel followed by 2 mL of 1.0 M DIPEA in DMF to initiate the coupling. The reaction vessel was then shaken for 30 min at 50°C; 4) DMF wash; 5) capping with 10% Ac_2O in 0.1 M DIPEA in DMF; 6) DMF wash; 7) DCM wash. Aliquots of resin of the obtained sequences were checked on an analytical Agilent Technologies 1260 Infinity system with a Gemini 3 µm, C18, 110 Å, 50 x 4.6 mm column or a Vydac 219TP 5 µm Diphenyl, 150 x 4.6 mm column with a 1 ml/min flow. The Fmoc amino acids applied in the synthesis were: Fmoc-Ala-OH, Fmoc-Asn(Trt)-OH, Fmoc-Asp(O*t*Bu)-OH, Fmoc-Gln(Trt)-OH, Fmoc-Glu(O*t*Bu)-OH, Fmoc-Gly-OH, Fmoc-Ile-OH, Fmoc-Leu-OH, Fmoc-Lys(Boc)-OH, Fmoc-Lys(MMT)-OH, Fmoc-Phe-OH, Fmoc-Ser(O*t*Bu)-OH Fmoc-Val-OH.

General procedure for cleavage from the resin, deprotection and purification. 30 µmol resin was washed with DMF, DCM and dried after the last synthesis step followed by a treatment for 180 minutes with 0.6 mL cleavage cocktail of 95% TFA, 2.5% TIS and 2.5% H_2O. The suspension was filtered, the resin was washed with 0.6 mL of the cleavage cocktail, and the combined TFA solutions were added dropwise to cold Et_2O and stored at -20°C overnight. The obtained suspension of the product in Et_2O was centrifuged, Et_2O was removed and the precipitant was dissolved in $CH_3CN/H_2O/$*t*BuOH (1/1/1 v/v/v) or DMSO/$CH_3CN/H_2O/$*t*BuOH (3/1/1/1 v/v/v/v). Purification was performed on a Gilson GX-281 preparative RP-HPLC with a Gemini-NX 5u, C18, 110 Å, 250 x 10.0 mm column or a Vydac 219TP 5 µm Diphenyl, 250 x 10 mm column.

General purification method for CRX-527-*O*-conjugates. A C18 column was washed subsequently with CH_3CN, MeOH, DCM/MeOH (1/1 v/v), MeOH, CH_3CN, CH_3CN/H_2O, H_2O. The reaction mixture was added on the column and the Eppendorf was rinsed with a mixture of $CH_3CN/$*t*BuOH/MilliQ H_2O (1/1/1 v/v/v, 0.50 mL), which was also added on the C18 column. The column was subsequent-

ly flushed with 6 mL of the follow solvent systems: H_2O, CH_3CN/H_2O (1/1 v/v), CH_3CN, DMSO, CH_3CN/*t*BuOH/MilliQ H_2O (1/1/1 v/v/v) and collected in Eppendorfs containing 1.0 mL of each solvent system. The column was then flush with MeOH (6.0 mL), followed by DCM/MeOH (1/1 v/v, 6.0 mL), which were collected in separate flasks, concentrated *in vacuo* at 35°C and lyophilized by dissolving in CH_3CN/*t*BuOH/MilliQ H_2O (1/1/1 v/v/v), yielding the conjugate as a white solid. *For the amide conjugates, H_2O + 0.1% TFA was used instead of H_2O.

MALDI-TOF measurements. MALDI-TOF measurements: 1 **µ**L of a DMSO solution of the compound was spotted on a 384-MTP target plate (Bruker Daltonics, Bremen, Germany) and air-dried. Subsequently 1 **µ**L of 2,5-dihydroxybenzoic acid (2,5-DHB; Bruker Daltonics) matrix (20 mg/mL in ACN/water; 50:50 (v/v)) was applied on the plate and the spots were left to dry prior MALDI-TOF analysis. An Ultraflextreme MALDI-TOF (Bruker Daltonics), equipped with Smartbeam-II laser was used to measure the samples in reflectron positive ion mode. The MALDI-TOF was calibrated using a peptide calibration standard prior to measurement.

Synthesis and Characterizations. The synthesis and characterizations for compounds **9, 10, 11, 12, 13, 15, 16a, 16b, 1, 2, 3, 4, 20a, 20b, 21, 22, 5, 6, 7, 8, 23, 14**, **17**, **18**, and **18**, can be found in the online version of the publication and in the online supplementary information.

Immunological evaluation procedures.

Cell culture. The D1 cell line is a growth factor-dependent immature spleen-derived DC cell line from C57BL/6 (H-2^b) mice. D1 and B3Z cells were cultured as described elsewhere.[55] The B3Z cell line was cultured in IMDM medium (Lonza, Basel, Switzerland) supplemented with 8% FCS (Greiner, Kremsmünster, Austria), penicillin and streptomycin, glutamine (Gibco, Carlsbad, CA, USA), β-mercaptoethanol (Merck, Kenilworth, NJ USA), and hygromycin B (AG Scientific Inc, San Diego, CA, USA) to maintain expression of the beta-galactosidase reporter gene.

In vitro DC maturation assay. The test compounds were dissolved in DMSO at a concentration of 500 µM and sonicated in water bath for 15 minutes. 50.000 D1 cell were seeded in 96-well round bottom plates (Corning, Amsterdam, The Netherlands) in 100 µl of R1 supplemented IMDM medium and 100 µl of 2 times concentrated test compounds in medium were added. After 24 hours of incubation at 37°C, supernatant was taken from the wells for ELISA analysis (BioLegend, San Diego, USA) to measure the amount of produced IL-12p40.

In vitro antigen presentation assay. The test compounds were dissolved in DMSO at a concentration of 500 µM and sonicated in water bath for 15 minutes. 50.000

D1 cells were seeded in 96-well flat bottom plates and pulsed for 2 hours with 200 µl of the test compounds in medium at the indicated concentrations. After 2 hours, cells were washed once with 200 µl of fresh medium and 50.000 B3Z were added per well in 200 µl of medium and incubated with the pulsed D1 cells overnight. The following day TCR activation was detected by measurement of absorbance at 595 nm upon color conversion of chlorophenol red-β-D-galacto-pyranoside (Calbiochem®, Merck, Bullington MA, USA) by the beta-galactosidase enzyme, followed by measurement of absorbance at 595 nm.[56,57]

Mice. Female C57BL/6 mice were purchased from Charles River Laboratories. Congenic CD45.1$^+$ C57BL/6 mice were bred at the Leiden University medical Centre animal facility. All animal experiments were in accordance with the Dutch national regulations and received ethical and technical approval by the local Animal Welfare Body.

Immunization of mice. 6-8 weeks old C57BL/6 female mice were injected intradermally at the tail base with 5 nmol of each conjugate or an equimolar mix of Lipid A and $DEVA_5K$ peptide. To prepare the vaccine, the different compounds were dissolved in DMSO at a concentration of 500 µM and sonicated in water bath for 15 minutes. The required amounts for vaccination was added to saline solution and 30 µl per mouse were injected. Fourteen days later, the animals were boosted with the same vaccine formulations. At different time points during the experiments, 20 µl of blood were collected from the tail vein for detection of SIINFEKL-specific T cell responses via SIINFEKL-H2-Kb tetramer staining. At the end of the experiments, spleens and lymph nodes were removed and processed in single cell suspensions for *ex vivo* analysis.

In vivo specific killing.Splenocytes were harvested from CD45.1$^+$ C57BL/6 naïve mice, processed into single cell suspension and labelled with either 5 or 0.005 µM CFSE for 10 min at 37°C. Cells that were labelled with 0.005 µM CFSE (CFSE low) were loaded for 1 hour at 37°C with 1µM SIINFEKL peptide, while cells that were labelled with 5 µM CFSE (CFSE high) were loaded in the same conditions with an irrelevant epitope derived from the E6 protein of Human Papilloma Virus (sequence: RAHYNIVTF). 4'000'000 splenocytes per peptide-loaded group were injected intravenously in vaccinated or naïve mice. One day after transfer, mice were sacrificed and the spleens were harvested and processed into single cell suspensions. Splenocytes were subsequently stained with eFluor®450 anti-CD45.1 antibody (eBioscience, San Diego, USA) and analyzed by flow cytometry to detect CD45.1$^+$/CFSE$^+$ target cells. Specific killing was calculated according to the following equation: Specific killing = 100 - [100*((CFSE target peptide)/(CFSE irrelevant) immunized mice)/((CFSE target peptide)/(CFSE irrelevant) naïve mice)]

REFERENCES

(1) Wei, S. C.; Duffy, C. R.; Allison, J. P. Fundamental Mechanisms of Immune Checkpoint Blockade Therapy. *Cancer Discovery*. **2018**, *8*, 1069–1086.

(2) Mchayleh, W.; Bedi, P.; Sehgal, R.; Solh, M. Chimeric Antigen Receptor T-Cells: The Future Is Now. *J. Clin. Med.* **2019**, *8*, 207.

(3) Schumacher, T. N.; Schreiber, R. D. Neoantigens in Cancer Immunotherapy. *Science*. **2015**, *348*, 69–74.

(4) Heimburg-Molinaro, J.; Lum, M.; Vijay, G.; Jain, M.; Almogren, A.; Rittenhouse-Olson, K. Cancer Vaccines and Carbohydrate Epitopes. *Vaccine* **2011**, *29*, 8802–8826.

(5) Brubaker, S. W.; Bonham, K. S.; Zanoni, I.; Kagan, J. C. Innate Immune Pattern Recognition: A Cell Biological Perspective. *Annu. Rev. Immunol.* **2015**, *33*, 257–290.

(6) Iwasaki, A.; Medzhitov, R. Toll-like Receptor Control of the Adaptive Immune Responses. *Nat. Immunol.* **2004**, *5*, 987–995.

(7) Kawai, T.; Akira, S. The Role of Pattern-Recognition Receptors in Innate Immunity: Update on Toll-like Receptors. *Nat. Immunol.* **2010**, *11*, 373–384.

(8) van Dinther, D.; Stolk, D. A.; van de Ven, R.; van Kooyk, Y.; de Gruijl, T. D.; den Haan, J. M. M. Targeting C-Type Lectin Receptors: A High-Carbohydrate Diet for Dendritic Cells to Improve Cancer Vaccines. *J. Leukoc. Biol.* **2017**, *102*, 1017–1034.

(9) Garaude, J.; Kent, A.; van Rooijen, N.; Blander, J. M. Simultaneous Targeting of Toll- and Nod-Like Receptors Induces Effective Tumor-Specific Immune Responses. *Sci. Transl. Med.* **2012**, *4*, 120ra16.

(10) Zom, G. G.; Willems, M. M. J. H. P.; Meeuwenoord, N. J.; Reintjens, N. R. M.; Tondini, E.; Khan, S.; Overkleeft, H. S.; van der Marel, G. A.; Codee, J. D. C.; Ossendorp, F.; Filippov, D. V. Dual Synthetic Peptide Conjugate Vaccine Simultaneously Triggers TLR2 and NOD2 and Activates Human Dendritic Cells. *Bioconjug. Chem.* **2019**, *30*, 1150–1161.

(11) Zom, G. G. P.; Khan, S.; Filippov, D. V.; Ossendorp, F. TLR Ligand–Peptide Conjugate Vaccines. In *Advances in Immunology*; **2012**, *114*, 177–201.

(12) Liu, H.; Irvine, D. J. Guiding Principles in the Design of Molecular Bioconjugates for Vaccine Applications. *Bioconjug. Chem.* **2015**, *26*, 791–801.

(13) Steinhagen, F.; Kinjo, T.; Bode, C.; Klinman, D. M. TLR-Based Immune Adjuvants. *Vaccine*. **2011**, *29*, 3341–3355.

(14) Dowling, J. K.; Mansell, A. Toll-like Receptors: The Swiss Army Knife of Immunity and Vaccine Development. *Clinical and Translational Immunology*. **2016**, 5:e85. https://doi.org/10.1038/cti.2016.22.

(15) Moyle, P. M.; Toth, I. Modern Subunit Vaccines: Development, Components, and Research Opportunities. *ChemMedChem* **2013**, *8*, 360–376.

(16) Ignacio, B. J.; Albin, T. J.; Esser-Kahn, A. P.; Verdoes, M. Toll-like Receptor Agonist Conjugation: A Chemical Perspective. *Bioconjug. Chem.* **2018**, *29*, 587–603.

(17) Ingale, S.; Wolfert, M. A.; Gaekwad, J.; Buskas, T.; Boons, G.-J. Robust Immune Responses Elicited by a Fully Synthetic Three-Component Vaccine. *Nat. Chem. Biol.* **2007**, *3*, 663–667.

(18) Khan, S.; Weterings, J. J.; Britten, C. M.; de Jong, A. R.; Graafland, D.; Melief, C. J. M.; van

der Burg, S. H.; van der Marel, G.; Overkleeft, H. S.; Filippov, D. V.; Ossendorp, F. Chirality of TLR-2 Ligand Pam3CysSK4 in Fully Synthetic Peptide Conjugates Critically Influences the Induction of Specific CD8+ T-Cells. *Mol. Immunol.* **2009**, *46*, 1084–1091.

(19) Abdel-Aal, A.-B. M.; Zaman, M.; Fujita, Y.; Batzloff, M. R.; Good, M. F.; Toth, I. Design of Three-Component Vaccines against Group A Streptococcal Infections: Importance of Spatial Arrangement of Vaccine Components. *J. Med. Chem.* **2010**, *53*, 8041–8046.

(20) Khan, S.; Bijker, M. S.; Weterings, J. J.; Tanke, H. J.; Adema, G. J.; van Hall, T.; Drijfhout, J. W.; Melief, C. J. M.; Overkleeft, H. S.; van der Marel, G. A.; Filippov, D. V.; van der Burg, S. H.; Ossendorp, F. Distinct Uptake Mechanisms but Similar Intracellular Processing of Two Different Toll-like Receptor Ligand-Peptide Conjugates in Dendritic Cells. *J. Biol. Chem.* **2007**, *282*, 21145–21159.

(21) Zom, G. G.; Willems, M. M. J. H. P.; Khan, S.; Van Der Sluis, T. C.; Kleinovink, J. W.; Camps, M. G. M.; Van Der Marel, G. A.; Filippov, D. V.; Melief, C. J. M.; Ossendorp, F. Novel TLR2-Binding Adjuvant Induces Enhanced T Cell Responses and Tumor Eradication. *J. Immunother. Cancer* **2018**, *6*, 146.

(22) Willems, M. M. J. H. P.; Zom, G. G.; Khan, S.; Meeuwenoord, N.; Melief, C. J. M.; van der Stelt, M.; Overkleeft, H. S.; Codée, J. D. C.; van der Marel, G. A.; Ossendorp, F.; Filippov, D. V. N -Tetradecylcarbamyl Lipopeptides as Novel Agonists for Toll-like Receptor 2. *J. Med. Chem.* **2014**, *57*, 6873–6878.

(23) Weterings, J. J.; Khan, S.; van der Heden, G. J.; Drijfhout, J. W.; Melief, C. J. M.; Overkleeft, H. S.; van der Burg, S. H.; Ossendorp, F.; van der Marel, G. A.; Filippov, D. V. Synthesis of 2-Alkoxy-8-Hydroxyadenylpeptides: Towards Synthetic Epitope-Based Vaccines. *Bioorg. Med. Chem. Lett.* **2006**, *16*, 3258–3261.

(24) Fujita, Y.; Hirai, K.; Nishida, K.; Taguchi, H. 6-(4-Amino-2-Butyl-Imidazoquinolyl)-Norleucine: Toll-like Receptor 7 and 8 Agonist Amino Acid for Self-Adjuvanting Peptide Vaccine. *Amino Acids* **2016**, *48*, 1319–1329.

(25) Kramer, K.; Young, S. L.; Walker, G. F. Comparative Study of 5′- and 3′-Linked CpG–Antigen Conjugates for the Induction of Cellular Immune Responses. *ACS Omega* **2017**, *2*, 227–235

(26) Daftarian, P.; Sharan, R.; Haq, W.; Ali, S.; Longmate, J.; Termini, J.; Diamond, D. J. Novel Conjugates of Epitope Fusion Peptides with CpG-ODN Display Enhanced Immunogenicity and HIV Recognition. *Vaccine* **2005**, *23*, 3453–3468.

(27) Alving, C. R.; Peachman, K. K.; Rao, M.; Reed, S. G. Adjuvants for Human Vaccines. *Curr. Opin. Immunol.* **2012**, *24*, 310–315.

(28) Casella, C. R.; Mitchell, T. C. Putting Endotoxin to Work for Us: Monophosphoryl Lipid A as a Safe and Effective Vaccine Adjuvant. *Cell. Mol. Life Sci.* **2008**, *65*, 3231–3240.

(29) Garçon, N.; Di Pasquale, A. From Discovery to Licensure, the Adjuvant System Story. *Hum. Vaccin. Immunother.* **2017**, *13*, 19–33.

(30) Wang, Q.; Zhou, Z.; Tang, S.; Guo, Z. Carbohydrate-Monophosphoryl Lipid A Conjugates Are Fully Synthetic Self-Adjuvanting Cancer Vaccines Eliciting Robust Immune Responses in the Mouse. *ACS Chem. Biol.* **2012**, *7*, 235–240.

(31) Zhou, Z.; Mondal, M.; Liao, G.; Guo, Z. Synthesis and Evaluation of Monophosphoryl Lipid A Derivatives as Fully Synthetic Self-Adjuvanting Glycoconjugate Cancer Vaccine Carriers. *Org. Biomol. Chem.* **2014**, *12*, 3238–

3245.

(32) Zhou, Z.; Liao, G.; Mandal, S. S.; Suryawanshi, S.; Guo, Z. A Fully Synthetic Self-Adjuvanting Globo H-Based Vaccine Elicited Strong T Cell-Mediated Antitumor Immunity. *Chem. Sci.* **2015**, *6*, 7112–7121.

(33) Liao, G.; Zhou, Z.; Suryawanshi, S.; Mondal, M. A.; Guo, Z. Fully Synthetic Self-Adjuvanting α-2,9-Oligosialic Acid Based Conjugate Vaccines against Group C Meningitis. *ACS Cent. Sci.* **2016**, *2*, 210–218.

(34) Wang, L.; Feng, S.; Wang, S.; Li, H.; Guo, Z.; Gu, G. Synthesis and Immunological Comparison of Differently Linked Lipoarabinomannan Oligosaccharide–Monophosphoryl Lipid A Conjugates as Antituberculosis Vaccines. *J. Org. Chem.* **2017**, *82*, 12085–12096.

(35) Zamyatina, A. Aminosugar-Based Immunomodulator Lipid A: Synthetic Approaches. *Beilstein J. Org. Chem.* **2018**, *14*, 25–53.

(36) Fujimoto, Y.; Shimoyama, A.; Saeki, A.; Kitayama, N.; Kasamatsu, C.; Tsutsui, H.; Fukase, K. Innate Immunomodulation by Lipophilic Termini of Lipopolysaccharide; Synthesis of Lipid As from Porphyromonas Gingivalis and Other Bacteria and Their Immunomodulative Responses. *Mol. Biosyst.* **2013**, *9*, 987.

(37) Li, Q.; Guo, Z. Recent Advances in Toll Like Receptor-Targeting Glycoconjugate Vaccines. *Molecules* **2018**, *23*, 1583.

(38) Stöver, A. G.; Da Silva Correia, J.; Evans, J. T.; Cluff, C. W.; Elliott, M. W.; Jeffery, E. W.; Johnson, D. A.; Lacy, M. J.; Baldridge, J. R.; Probst, P.; Ulevitch, R. J.; Persing, D. H.; Hershberg, R. M. Structure-Activity Relationship of Synthetic Toll-like Receptor 4 Agonists. *J. Biol. Chem.* **2004**, *279*, 4440–4449.

(39) Cluff, C. W.; Baldridge, J. R.; Stover, A. G.; Evans, J. T.; Johnson, D. A.; Lacy, M. J.; Clawson, V. G.; Yorgensen, V. M.; Johnson, C. L.; Livesay, M. T.; Hershberg, R. M.; Persing, D. H. Synthetic Toll-Like Receptor 4 Agonists Stimulate Innate Resistance to Infectious Challenge. *Infect. Immun.* **2005**, *73*, 3044–3052.

(40) Bazin, H. G.; Bess, L. S.; Livesay, M. T.; Ryter, K. T.; Johnson, C. L.; Arnold, J. S.; Johnson, D. A. New Synthesis of Glycolipid Immunostimulants RC-529 and CRX-524. *Tetrahedron Lett.* **2006**, *47*, 2087–2092.

(41) Bazin, H. G.; Murray, T. J.; Bowen, W. S.; Mozaffarian, A.; Fling, S. P.; Bess, L. S.; Livesay, M. T.; Arnold, J. S.; Johnson, C. L.; Ryter, K. T.; Cluff, C. W.; Evans, J. T., Johnson, D. A. The 'Ethereal' Nature of TLR4 Agonism and Antagonism in the AGP Class of Lipid A Mimetics. *Bioorg. Med. Chem. Lett.* **2008**, *18*, 5350–5354.

(42) Dupont, J.; Altclas, J.; Lepetic, A.; Lombardo, M.; Vázquez, V.; Salgueira, C.; Seigelchifer, M.; Arndtz, N.; Antunez, E.; von Eschen, K.; Janowicz, Z. A Controlled Clinical Trial Comparing the Safety and Immunogenicity of a New Adjuvanted Hepatitis B Vaccine with a Standard Hepatitis B Vaccine. *Vaccine* **2006**, *24*, 7167–7174.

(43) Park, B. S.; Lee, J.-O. Recognition of Lipopolysaccharide Pattern by TLR4 Complexes. *Exp. Mol. Med.* **2013**, *45*, e66.

(44) DeMarco, M. L.; Woods, R. J. From Agonist to Antagonist: Structure and Dynamics of Innate Immune Glycoprotein MD-2 upon Recognition of Variably Acylated Bacterial Endotoxins. *Mol. Immunol.* **2011**, *49* , 124–133.

(45) Trinchieri, G. Interleukin-12 and the Regulation of Innate Resistance and Adaptive Immunity. *Nat. Rev. Immunol.* **2003**, *3*, 133–146.

(46) van Duikeren, S.; Fransen, M. F.; Redeker, A.; Wieles, B.; Platenburg, G.; Krebber,

W.-J.; Ossendorp, F.; Melief, C. J. M.; Arens, R. Vaccine-Induced Effector-Memory CD8 + T Cell Responses Predict Therapeutic Efficacy against Tumors. *J. Immunol.* **2012**, *189*, 3397–3403.

(47) Butler, N. S.; Nolz, J. C.; Harty, J. T. Immunologic Considerations for Generating Memory CD8 T Cells through Vaccination. *Cellular Microbiology*. **2011**, *13*, 925–933.

(48) Seaman, M. S.; Peyerl, F. W.; Jackson, S. S.; Lifton, M. A.; Gorgone, D. A.; Schmitz, J. E.; Letvin, N. L. Subsets of Memory Cytotoxic T Lymphocytes Elicited by Vaccination Influence the Efficiency of Secondary Expansion In Vivo. *J. Virol.* **2004**, *78*, 206–215.

(49) Borowski, A. B.; Boesteanu, A. C.; Mueller, Y. M.; Carafides, C.; Topham, D. J.; Altman, J. D.; Jennings, S. R.; Katsikis, P. D. Memory CD8 + T Cells Require CD28 Costimulation . *J. Immunol.* **2007**, *179*, 6494–6503.

(50) Mousavi, S. F.; Soroosh, P.; Takahashi, T.; Yoshikai, Y.; Shen, H.; Lefrançois, L.; Borst, J.; Sugamura, K.; Ishii, N. OX40 Costimulatory Signals Potentiate the Memory Commitment of Effector CD8 + T Cells . *J. Immunol.* **2008**, *181*, 5990–6001.

(51) Shedlock, D. J.; Shen, H. Requirement for CD4 T Cell Help in Generating Functional CD8 T Cell Memory. *Science*. **2003**, *300*, 337–339.

(52) Janssen, E. M.; Lemmens, E. E.; Wolfe, T.; Christen, U.; Von Herrath, M. G.; Schoenberger, S. P. CD4+ T Cells Are Required for Secondary Expansion and Memory in CD8+ T Lymphocytes. *Nature* **2003**, *421*, 852–856.

(53) Ahrends, T.; Busselaar, J.; Severson, T. M.; Bąbała, N.; de Vries, E.; Bovens, A.; Wessels, L.; van Leeuwen, F.; Borst, J. CD4+ T Cell Help Creates Memory CD8+ T Cells with Innate and Help-Independent Recall Capacities. *Nat. Commun.* **2019**, *10*, 5531.

(54) Paquet, A. Introduction of 9-Fluorenylmethyloxycarbonyl, Trichloroethoxycarbonyl, and Benzyloxycarbonyl Amine Protecting Groups into O-Unprotected Hydroxyamino Acids Using Succinimidyl Carbonates. *Can. J. Chem.* **1982**, *60*, 976–980.

(55) Winzler, C.; Rovere, P.; Zimmermann, V. S.; Davoust, J.; Rescigno, M.; Citterio, S.; Ricciardi-Castagnoli, P. Checkpoints and Functional Stages in DC Maturation. *Adv. Exp. Med. Biol.* **1997**, *417*, 59–64.

(56) Sanderson, S.; Shastri, N. LacZ Inducible, Antigen/MHC-Specific T Cell Hybrids. *Int. Immunol.* **1994**, *6*, 369–376.

(57) Schuurhuis, D. H.; Ioan-Facsinay, A.; Nagelkerken, B.; van Schip, J. J.; Sedlik, C.; Melief, C. J. M.; Verbeek, J. S.; Ossendorp, F. Antigen-Antibody Immune Complexes Empower Dendritic Cells to Efficiently Prime Specific CD8 + CTL Responses In Vivo. *J. Immunol.* **2002**, *168*, 2240–2246.